

Vascular Targeting of Ocular Neovascularization with a VEGF₁₂₁/Gelatin Chimeric Protein

Hideo Akiyama, Khalid A. Mohamedali, Raquel Lima e Silva, Shu Kachi, JiKui Shen, Christina Hata, Naoyasu Umeda, Sean F. Hackett, Sadia Aslam, Melissa Krause, Hong Lai, Michael G. Rosenblum, Peter A. Campochiaro

¹The Departments of Ophthalmology and Neuroscience (HA, RLS, SK, JS, CH, NU, SFH, SA, MK, HL, PAC)
The Johns Hopkins University School of Medicine
Maumenee 719
600 N. Wolfe Street
Baltimore, Maryland 21287-9277

²Immunopharmacology and Targeted Therapy Section (KAM, MGR)
Department of Experimental Therapeutics
M. D. Anderson Cancer Center
1515 Holcombe Boulevard
Houston, TX 77030-4009

This study was supported by PHS grants EY05951, EY10017, and core grant P30EY1765 from the National Eye Institute, a grant from the Macula Vision Research Foundation and a grant from Dr. and Mrs. William Lake. Research conducted, in part, by the Clayton Foundation for Research. PAC is the George S. and Dolores Dore Eccles Professor of Ophthalmology and Neuroscience.

Running Title Page

Running Title: Targeted toxin-induced regression of ocular neovascularization

Address correspondence to: Peter A. Campochiaro, M.D.
Maumenee 719
The Johns Hopkins University School of Medicine
600 N. Wolfe Street
Baltimore, MD 21287-9277
Telephone #: (410) 955-5106
Fax #: (410) 614-9315
E Mail: pcampo@jhmi.edu

Text pages- 15

Tables- 0

Figures- 5

References- 40

Word Counts: Abstract- 187

Introduction- 373

Discussion- 443

Abbreviations: vascular endothelial growth factor, VEGF; VEGF/recombinant gelonin chimeric protein, VEGF/rGel; prostate-specific membrane antigen, PSMA; vascular cell adhesion molecule-1; VCAM-1, phosphate-buffered saline (PBS); transgenic mice in which the rhodopsin promoter drives expression of VEGF in photoreceptors; rho/VEGF mice, *Griffonia simplicifolia* lectin B4, GSA.

Abstract

Tumors provide an extremely abnormal microenvironment that stimulates neovascularization from surrounding vessels and causes altered gene expression within vascular cells. Upregulation of vascular endothelial growth factor (VEGF) receptors has allowed selective destruction of tumor vessels by administration of a chimeric protein consisting of VEGF₁₂₁ coupled to the toxin gelonin (VEGF/rGel). We sought to determine if there is sufficient upregulation of VEGF receptors in endothelial cells participating in ocular neovascularization to permit a similar strategy. After intravenous injection of 45 mg/kg of VEGF/rGel, but not uncoupled rGel, there was immunofluorescent staining for rGel within choroidal neovascularization in mice and regression of the neovascularization occurred demonstrating successful vascular targeting via the systemic circulation. Intraocular injection of 5 ng of VEGF/rGel also caused significant regression of choroidal neovascularization and regression of retinal neovascularization in two models, transgenic mice with expression of VEGF in photoreceptors and mice with ischemic retinopathy, while injection of 5 ng of rGel had no effect. These data suggest that the strategy of vascular targeting can be applied to non-malignant neovascular diseases and could serve as the basis of a new treatment to reduce established ocular neovascularization.

Introduction

As tumors grow, they become hypoxic causing increased production of VEGF and other hypoxia-regulated gene products (Plate et al., 1992; Shweiki et al., 1992). Angiogenesis is stimulated from surrounding host vessels and the new vessels invade and vascularize the tumor. Despite vascularization and elimination of some of the hypoxia, tumors provide a very abnormal environment for their vasculature. Tumors release several vasoactive substances and disturb cell-cell and cell-matrix interactions. Tumor cells may become incorporated among endothelial cells (Chang et al., 2000) and in other areas defects between endothelial cells result in severe leakiness (Hahizume et al., 2000). Excessive exposure of abluminal surfaces to serum components perturbs the basement membrane of vascular cells, a major determinant of phenotype and behavior of cells (Baluk et al., 2003). The altered microenvironment results in differential gene expression resulting in markers for tumor vasculature, including integrins $\alpha_v\beta_3$ and $\alpha_v\beta_5$ (Brooks et al., 1994), the ED-B domain of fibronectin (Zardi et al., 1987), and prostate-specific membrane antigen (PSMA) (Liu et al., 1997), just to name a few. Some gene products, such as VEGF receptors, that are present at low levels in normal endothelial cells, are substantially more abundant in endothelium of tumor vessels (Plate et al., 1993). Recently, a variety of techniques such as *in vivo* screening of phage-displayed peptide libraries (Pasqualini and Ruoslahti, 1996), serial analysis of gene expression (Carson-

Walter et al., 2001), and proteomic analyses (Oh et al., 2004; Schnitzer, 1998) have greatly expanded the list of potential markers for tumor vasculature.

Differentially expressed gene products provide a means to direct therapeutic agents to tumor vasculature, a strategy that is commonly referred to as “vascular targeting” (Denekamp, 1984; Denekamp, 1999; Thorpe, 2004). Tumor vessel markers that have been exploited and demonstrated to have therapeutic potential in tumor models include (but are not limited to), $\alpha_v\beta_3$ and $\alpha_v\beta_5$ integrins (Pasqualini et al., 1997), VEGF receptors (Arora et al., 1999; Liu et al., 2003; Ramakrishnan et al., 1996; Veenendaal et al., 2002), the ED-B domain of fibronectin (Nilsson et al., 2001), VCAM-1 (Ran et al., 1998), and PSMA (Liu et al., 2002).

Endothelial cells participating in angiogenesis in disease processes other than tumors also display differential gene expression. For instance, there is substantial upregulation of $\alpha_v\beta_3$ in ischemia-induced retinal neovascularization (Luna et al., 1996). However, ocular neovascularization may not differ from normal vessels to the same degree as tumor vasculature and it is not known if the strategy of vascular targeting can be applied to ocular neovascularization. In this study, we tested in several models of ocular neovascularization the effects of systemic or intraocular administration of a VEGF₁₂₁/gelonin chimeric protein (VEGF/rGel), which has previously been shown to cause infarction of tumor vessels (Veenendaal et al., 2002).

Materials and Methods

Materials

The fusion toxin, VEGF/rGel, and recombinant gelonin (rGel) were expressed in bacterial cultures, purified to homogeneity and characterized for biological activity as previously described (Veenendaal et al., 2002). The fusion toxin and rGel were stored in phosphate-buffered saline (PBS) at -20°C.

Model of choroidal neovascularization

Mice were treated in accordance with the ARVO Statement for the Use of Animals in Ophthalmic and Vision Research and the U.S. National Institutes of Health Guide for the Care and Use of Laboratory Animals. The model of laser-induced choroidal neovascularization has been previously described (Tobe et al., 1998b). Briefly, 4- to 6-week-old female C57BL/6J mice were anesthetized with ketamine hydrochloride (100 mg/kg body weight) and xylazine hydrochloride (20/mg/kg), and pupils were dilated with 1% tropicamide. A 532 nm diode laser photocoagulator (OcuLight GL; Iridex, Mountain View, CA) with a slit lamp delivery system was used with a cover slip as a contact lens to visualize the retina and deliver sufficient laser energy (75 μ m spot size, 0.1 seconds duration, 140 mW) to rupture Bruch's membrane in 3 locations in each eye, the 9, 12, and 3 o'clock positions of the posterior pole. Production of a bubble at the time of laser burn, which indicates rupture of Bruch's membrane, is an important factor in

obtaining experimental CNV (Tobe et al., 1998b); therefore, only burns in which a bubble was produced were included in the study.

One week after rupture of Bruch's membrane, 7 mice were anesthetized and perfused with fluorescein-labeled dextran (2×10^6 average mw, Sigma, St. Louis, MO) and the amount of choroidal neovascularization at Bruch's membrane rupture sites was measured on choroidal flat mounts. Other mice received experimental or control injections one week after rupture of Bruch's membrane and choroidal neovascularization was assessed one week later. To test the effect of intravenous administration of VEGF/rGel, mice were given tail vein injections (every 2 days for a total of 4 injections) of 45 mg/kg of VEGF/rGel (8 mice) or rGel (8 mice), or PBS vehicle alone (7 mice). One week later, they were perfused with fluorescein-labeled dextran and choroidal neovascularization was measured on choroidal flat mounts. To test the effect of intravitreal administration of VEGF/rGel, 9 mice were given an intravitreal injection of 5 ng of rGel in one eye and PBS in the fellow eye and 13 mice were given 5 ng of VEGF/rGel in one eye and PBS in the fellow eye. After one week, mice were perfused with fluorescein-labeled dextran and choroidal neovascularization was measured on choroidal flat mounts.

Rho/VEGF transgenic mice

Transgenic mice in which the rhodopsin promoter drives expression of VEGF in photoreceptors (rho/VEGF mice) have been previously described (Okamoto et al., 1997; Tobe et al., 1998a). Hemizygous rho/VEGF (line V6)

transgenics in a C57BL/6 background were used for all experiments. At P21, the baseline amount of subretinal neovascularization was measured in eight mice. Nine mice received intravitreal injections at P21; 5 ng of VEGF/rGel was injected in one eye and 5 ng of rGel was injected in the other eye. At P25, the amount of subretinal neovascularization was measured in each eye.

Quantification of neovascularization on flat mounts

In mice with laser-induced choroidal neovascularization, the neovascularization was measured on choroidal flat mounts and in rho/VEGF transgenics, subretinal neovascularization was measured on retinal flat mounts. Flat mounts were prepared as previously described (Nambu et al., 2003; Tobe et al., 1998a). After mice were terminally perfused with fluorescein-labeled dextran, eyes were removed, fixed for 1 hour in 10% phosphate-buffered formalin, and the cornea and lens were removed. The entire retina was carefully dissected from the eyecup, and depending upon the model, the retina or choroid was flat mounted in Aquamount after 4 radial cuts were made in each quadrant. Flat mounts were examined by fluorescence microscopy using an Axioskop II microscope (Zeiss, Thornwood, NY) and captured with a Cool Snap-Pro digital color camera (Photometrics, Tucson, AZ). Retinas were mounted with photoreceptor side up and examined with 400x magnification, which provides a narrow depth of field so that when focusing on the outer edge of the retina the retinal vessels are out-of-focus in the background allowing easy delineation of the subretinal neovascularization. Image-Pro Plus software (Media Cybernetics,

Silver Spring, MD) was used to measure the area of each subretinal or choroidal neovascularization lesion.

Quantitative real time RT-PCR

Adult C57BL/6 mice had laser-induced rupture of Bruch's membrane in 3 locations in one eye and the contralateral eye served as control. After 1 week, mice were euthanized and eyes were removed. Anterior segments and retinas were removed and eyecups, which contain the choroid, were snap frozen by placing them into a mortar pre-cooled with liquid nitrogen, crushed, and the frozen powder was transferred into 1.5 ml tubes filled with 0.6 ml of lysis buffer. Rho/VEGF transgenic mice and littermate controls were euthanized at P16, and retinas which contain the retinal neovascularization, were isolated, snap frozen, pulverized, and placed in lysis buffer.

RNA isolation was performed using an RNeasy kit (QIAGEN Inc., Chatsworth, California, USA). To remove any contaminating genomic DNA, RNA samples were treated with DNase I (Invitrogen, California, USA) at room temperature for 15 minutes and then cDNA was synthesized with reverse transcriptase (SuperScript III; Life Technologies, Gaithersburg, MD) and 5 μ M random hexamer. Real time quantitative PCR was performed and analyzed on the MJ Research Chrom4 Thermal Cycler System (MJ Research Inc., Waltham, MA) using the SYBR Green I format. Reactions were performed in a 20 μ l volume using the SYBR Green reaction mixture (QIAGEN Inc., Chatsworth, California, USA) with 0.5 mM primers. 28S rRNA was used as a standard for

normalization. The sequences of the PCR primer pairs were: (1) VEGF receptor 2, 5'-CAC CTG CCA GGC CTG CAA-3' (forward), 5'-GCT TGG TGC AGG CGC CTA-3' (reverse), and (2) 28S, 5'-TTG AAA ATC CGG GGG AGA G-3' (forward) and 5'-ACA TTG TTC CAA CAT GCC AG-3' (reverse). Murine cDNA for VEGF receptor 2 and 28S rRNA were synthesized by RT-PCR from mouse retinal RNA using Pfu Taq polymerase (Stratagene, La Jolla, California). The PCR products were purified with a Qiagen gel extraction kit and used to generate standard curves for each gene for each real time PCR reaction. Standard curves were used to calculate mRNA copy numbers for each retinal RNA sample and target gene mRNA copy numbers were normalized to 10^7 copies of 28S.

Immunofluorescent localization of VEGF/rGel

One week after rupture of Bruch's membrane, mice were given 45 mg/kg of VEGF/rGel or rGel, or vehicle alone by tail vein injection. Forty-five minutes later, mice were given an intraperitoneal injection of 300 U of heparin and 15 minutes later, mice were terminally perfused by pumping saline into the left ventricle at 1 ml/minute for 12 minutes. Eyes were removed and frozen in optimum cutting temperature embedding compound (Miles Diagnostics, Elkhart, IN). Frozen sections were cut and adjacent sections were stained with biotinylated *Griffonia simplicifolia* lectin B4 (GSA), which selectively stains vascular cells, or 10 µg/ml of rabbit anti-rGel antibody (Veenendaal et al., 2002). Rabbit anti-rGel antibody was detected with goat anti-rabbit IgG conjugated to FITC (Jackson ImmunoResearch, West Grove, PA).

Histochemical Staining with GSA Lectin

Slides were incubated in methanol/H₂O₂ for 10 minutes at 4°C, washed with 0.05 M TBS and incubated for 30 minutes in 10% normal porcine serum (NPS). Slides were incubated 2 hours at room temperature with 1:20 biotinylated GSA lectin (Vector Laboratories, Burlingame, CA) in TBS/1% NPS and after rinsing with 0.05 M TBS, they were incubated with 1:10 avidin coupled to peroxidase (Vector Laboratories) in TBS/1% NPS for 45 minutes at room temperature. After a 10-minute wash in 0.05 M TBS, slides were incubated with diaminobenzidine (Research Genetics, Huntsville, AL) to produce a brown reaction product.

Mice with oxygen-induced ischemic retinopathy

Ischemic retinopathy was produced by a previously described method (Smith et al., 1994). At P7, litters of mice were placed in an airtight incubator and exposed to an atmosphere of 75 ± 3% oxygen for 5 days. Incubator temperature was maintained at 23 ± 2°C, and oxygen was measured every 8 hours with an oxygen analyzer. After 5 days, the mice were removed from the incubator and placed in room air. At P17, six mice were euthanized to measure the baseline amount of neovascularization and seven mice were given an intravitreal injection of 5 ng of VEGF/rGel in one eye and 5 ng of rGel in the other eye. At P21, mice were euthanized to measure retinal neovascularization.

Measurement of retinal neovascularization in mice with ischemic retinopathy

After euthanasia, eyes were rapidly removed and frozen in optimal cutting temperature embedding compound. Ocular frozen sections (10 μ m) were histochemically stained with GSA, as described above. Slides were counterstained with eosin, which stains the internal limiting membrane, and mounted (Cytoseal; Stephens Scientific, Cornwall, NJ). To perform quantitative assessments, 10 μ m serial sections were cut through the entire eye starting with sections that included the iris root on one side of the eye and proceeding to the iris root on the other side. Every tenth section, roughly 100 μ m apart, was stained with GSA and images were digitized with a three CCD color video camera and a frame grabber. Image analysis was used to delineate GSA-stained cells on the surface of the retina, and their area was measured. The mean area of neovascularization per section was calculated for each eye and was used as a single experimental value.

Statistical analyses

Statistical comparisons were made using a linear mixed model (Verbeke and Molenberghs, 2000). This model is analogous to analysis of variance (ANOVA), but allows analysis of all choroidal neovascularization area measurements from each mouse rather than average choroidal neovascularization area per mouse by accounting for correlation between measurements from the same mouse. The advantage of this model over

ANOVA is that it accounts for differing precision in mouse-specific average measurements arising from a varying number of observations among mice.

Results

VEGF receptor 2 is upregulated in choroidal and subretinal neovascularization

Seven days after rupture of Bruch's membrane in several locations, C57BL/6 mice were euthanized and total RNA was isolated from the eyecup. Compared to contralateral eyes that did not receive laser, quantitative RT-PCR demonstrated a significant increase in *VEGF receptor 2* mRNA in the retina/choroid of mice with choroidal neovascularization (Figure 1). Mice that carry a rhodopsin promoter/VEGF transgene spontaneously develop subretinal neovascularization (Okamoto et al., 1997). Compared to littermate transgene-negative controls, transgenic mice with subretinal neovascularization showed a large increase in *VEGF receptor 2* mRNA (Figure 1).

VEGF/rGel localizes to choroidal neovascularization after intravenous injection

Seven days after laser-induced rupture of Bruch's membrane, mice were given 45 mg/kg of rGel or VEGF/rGel, or vehicle alone by tail vein injection. After 1 hour the mice were euthanized and ocular sections were histochemically stained with GSA or immunofluorescently stained with anti-gelonin antibody. Mice that had received an injection of PBS or rGel showed choroidal neovascularization at Bruch's membrane rupture sites (Figures 2A and C, arrows) that did not stain for gelonin (Figures 2B and D, arrows). In contrast,

mice that had received an intravenous injection of VEGF/rGel showed staining for gelonin within choroidal neovascularization (Figure 2E and F, arrows).

Intravenous injection of VEGF/rGel causes regression of choroidal neovascularization

Thirty adult C57BL/6 mice had laser-induced rupture of Bruch's membrane in three locations in each eye. After 1 week, 7 mice were perfused with fluorescein-labeled dextran and the baseline amount of choroidal neovascularization at rupture sites (Figure 3A, arrows) was measured by image analysis of choroidal flat mounts. The remaining mice received tail vein injections every 2 days (4 injections) of 45 mg/kg of rGel or VEGF/rGel, or PBS. One week after the start of injections the mice were perfused with fluorescein-labeled dextran and choroidal flat mounts were examined by fluorescence microscopy. The area of choroidal neovascularization ($\text{mm}^2 \times 10^{-2}$) at rupture sites appeared smaller in mice that had been injected with VEGF/rGel (0.95 ± 0.20 , Figure 3D, arrows) compared to those in mice that had been injected with rGel (2.25 ± 0.30 , Figure 3B, arrows) or PBS (2.65 ± 0.48 , Figure 3C, arrows), and a statistically significant difference was confirmed by image analysis (Figure 3E). They were also smaller than baseline choroidal neovascularization lesions present on day 7 (1.56 ± 0.14 , Figure 3A and E), indicating that VEGF/rGel caused regression of choroidal neovascularization.

Intravitreal injection of VEGF/rGel causes regression of choroidal neovascularization

Thirty-one adult C57BL/6 mice had laser-induced rupture of Bruch's membrane in three locations in each eye. After 1 week, 9 mice were perfused with fluorescein-labeled dextran, choroidal flat mounts were prepared, and the baseline amount of choroidal neovascularization at rupture sites (Figure 4A) was measured. The remaining mice were divided into 2 groups; 9 mice received an intravitreal injection of 5 ng of rGel in one eye and PBS in the fellow eye and 13 mice received 5 ng of VEGF/rGel in one eye and PBS in the fellow eye. After 1 week, the mice were perfused with fluorescein-labeled dextran and choroidal flat mounts were examined by fluorescence microscopy. The area of choroidal neovascularization ($\text{mm}^2 \times 10^{-2}$) at rupture sites was less in mice that had been injected with VEGF/rGel (0.43 ± 0.07 ; Figure 4D, arrows and E) compared to that in mice that had been injected with rGel (1.03 ± 0.17 ; Figure 4B, arrows) or PBS (0.92 ± 0.20 ; Figure 4C, arrows). It was also smaller than the amount of choroidal neovascularization seen at baseline (1.19 ± 0.19 ; Figure 4A).

Intravitreal injection of VEGF/rGel causes regression of neovascularization in rho/VEGF transgenic mice

Transgenic mice in which the rhodopsin promoter drives expression of VEGF in photoreceptors (rho/VEGF mice) develop subretinal neovascularization that is quite consistent among mice of the same line in the same genetic background and is easily quantified by image analysis of retinal flat mounts after perfusion of mice with fluorescein-labeled dextran (Okamoto et al., 1997; Tobe et al., 1998a). Eight hemizygous rho/VEGF mice in a C57BL/6 background had the

baseline amount of neovascularization per retina ($\text{mm}^2 \times 10^{-3}$) measured at P21 (Figure 5A; 10.8 ± 1.7). The remainder of the transgenic mice ($n = 9$) received an intravitreal injection of 5 ng of rGel in one eye and 5 ng of VEGF/rGel in the fellow eye at P21. At P25, compared to the baseline area of neovascularization per retina at P21, the area of neovascularization per retina in VEGF/rGel mice (Figure 5C, 2.80 ± 0.98) was significantly less (Figure 5D). It was also significantly less than the area of neovascularization per retina seen in rGel-injected mice (8.81 ± 1.94 , Figure 5B and D).

Intravitreal injection of VEGF/rGel causes regression of ischemia induced retinal NV

Mice with oxygen-induced ischemic retinopathy have retinal neovascularization on the surface of the retina similar to that seen in patients with proliferative diabetic retinopathy or retinopathy of prematurity. In this model the amount of neovascularization is fairly stable between P17 and P21 and then regresses spontaneously. There was prominent neovascularization on the surface of the retina at P17 (Figure 6A and B). Eyes that received an intravitreal injection of rGel at P17 still showed substantial neovascularization on the surface of the retina at P21 (Figures 6C and D, arrows). However, mice that had been injected with VEGF/rGel at P17 showed almost no identifiable neovascularization at P21 (Figures 6E and F). Image analysis demonstrated that VEGF/rGel-injected mice had significantly less neovascularization ($0.93 \pm 0.25 \text{ mm}^2 \times 10^{-2}$) than mice injected with rGel (5.01 ± 0.46), and significantly less than

the baseline amount seen at P17 prior to injection (6.53 ± 0.42 , Figure 6G),
indicating that VEGF/rGel induced regression of the retinal neovascularization.

Discussion

Striking regression of tumors has been achieved in several mouse models by systemic injection of chimeric proteins consisting of a toxin coupled to a homing protein that binds to a gene product that is differentially expressed in tumor vasculature (Arora et al., 1999; Liu et al., 2002; Liu et al., 2003; Nilsson et al., 2001; Pasqualini et al., 1997; Ramakrishnan et al., 1996; Ran et al., 1998; Veenendaal et al., 2002). In this study, we have shown that there is upregulation of VEGF receptor 2 in subretinal or choroidal neovascularization allowing the same strategy can be used to treat these benign disease processes. Systemically injected VEGF/rGel localizes to choroidal neovascularization and causes significant regression of the neovascularization. As a relatively confined compartment, the eye also affords a modified approach in which VEGF/rGel is injected into the vitreous cavity. In three different models of ocular neovascularization, laser-induced rupture of Bruch's membrane, rho/VEGF transgenic mice, and oxygen-induced ischemic retinopathy, intravitreal injection of VEGF/rGel, but not injection of rGel, resulted in significant regression of neovascularization. Minimizing systemic exposure is a potential advantage and compared to systemic administration, intravitreal injection reduced the amount of VEGF/rGel required for treatment by approximately 1.8×10^5 -fold, another significant advantage, because production and purification of clinical grade recombinant proteins is expensive.

Ocular neovascularization is one of the most prevalent causes of visual morbidity in developed countries. Retinal neovascularization occurs in ischemic retinopathies such as diabetic retinopathy and is a major cause of visual loss in working age patients (Klein et al., 1984). Choroidal neovascularization occurs as a complication of age-related macular degeneration and is a major cause of visual loss in elderly patients. Improved treatments are needed to reduce the high rate of visual loss, and their development is likely to be facilitated by greater understanding of the molecular pathogenesis of ocular neovascularization. Several lines of evidence have suggested that VEGF is an important stimulator for both retinal and choroidal neovascularization (Adamis et al., 1994; Aiello et al., 1994; Aiello et al., 1995; Kwak et al., 2000; Ozaki et al., 2000; Saishin et al., 2003; Seo et al., 1999). This has led to clinical trials testing the effect of VEGF antagonists in patients with subfoveal choroidal neovascularization. Intraocular injections of pegaptanib, an aptamer that binds VEGF, every 6 weeks for 1 year reduced loss of vision compared to sham injections (Gragoudas et al., 2004). Slowing visual loss is an important achievement, but it is not the ultimate goal, which is to improve vision and/or maintain it within a range that permits optimal functioning.

In animal models, VEGF antagonists are very good at suppressing growth of neovascularization and reducing excessive leakage (Adamis et al., 1996; Aiello et al., 1995; Kwak et al., 2000; Ozaki et al., 2000; Saishin et al., 2003; Seo et al., 1999), but fail to cause regression of new vessels (unpublished data). This is supported by observations in patients with choroidal neovascularization treated

with VEGF antagonists in whom leakage is reduced, but the choroidal neovascularization is not eliminated (Gragoudas et al., 2004). Regression of neovascularization is likely to be needed to achieve optimal results. Systemic or intraocular administration of VEGF/rGel to achieve regression of neovascularization combined with a VEGF antagonist to prevent recurrence is an appealing strategy that deserves investigation.

References

- Adamis AP, Miller JW, Bernal M-T, D'Amico DJ, Folkman J, Yeo T-K and Yeo K-T (1994) Increased vascular endothelial growth factor levels in the vitreous of eyes with proliferative diabetic retinopathy. *Am. J. Ophthalmol.* **118**:445-450.
- Adamis AP, Shima DT, Tolentino MJ, Gragoudas ES, Ferrara N, Folkman J, D'Amore PA and Miller JW (1996) Inhibition of vascular endothelial growth factor prevents retinal ischemia-associated iris neovascularization. *Arch. Ophthalmol.* **114**:66-71.
- Aiello LP, Avery RL, Arrigg PG, Keyt BA, Jampel HD, Shah ST, Pasquale LR, Thieme H, Iwamoto MA, Park JE, Nguyen MS, Aiello LM, Ferrara N and King GL (1994) Vascular endothelial growth factor in ocular fluid of patients with diabetic retinopathy and other retinal disorders. *N. Engl. J. Med.* **331**:1480-1487.
- Aiello LP, Pierce EA, Foley ED, Takagi H, Chen H, Riddle L, Ferrara N, King GL and Smith LEH (1995) Suppression of retinal neovascularization in vivo by inhibition of vascular endothelial growth factor (VEGF) using soluble VEGF-receptor chimeric proteins. *Proc. Natl. Acad. Sci. U.S.A.* **92**:10457-10461.

- Arora N, Masood R, Zheng T, Cai J, Smith DL and Gill PS (1999) Vascular endothelial growth factor chimeric toxin is highly active against endothelial cells. *Canc. Res.* **59**:183-188.
- Baluk P, Morikawa S, Haskell A, Mancuso M and McDonald DM (2003) Abnormalities of basement membrane on blood vessels and endothelial sprouts in tumors. *Am. J. Pathol.* **163**:1801-1815.
- Brooks P, Clark R and Cheresh D (1994) Requirement of vascular integrin α -v β -3 for angiogenesis. *Science* **264**:569-571.
- Carson-Walter EB, Watkins DN, Nanda A, Vogelstein B and Kinzler KW (2001) Cell surface tumor endothelial markers are conserved in mice and humans. *Canc. Res.* **61**:6649-6655.
- Chang YS, di Tomaso E, McDonald DM, Jones R, Jain RK and Munn LL (2000) Mosaic blood vessels in tumors: Frequency of cancer cells in contact with flowing blood. *Proc Natl Acad Sci U S A* **97**:14608-14613.
- Denekamp J (1984) Vascular endothelium as the vulnerable element in tumours. *Acta Radiol. Oncol.* **23**:217-225.
- Denekamp J (1999) The tumour microcirculation as a target in cancer therapy: a clearer perspective. *Eur. J. Clin. Invest.* **29**:733-736.
- Gragoudas ES, Adamis AP, Cunningham ET, Jr., Feinsod M and Guyer DR (2004) Pegaptanib for neovascular age-related macular degeneration. *N. Eng. J. Med.* **351**:2805-2816.

- Hazhizume H, Baluk P, McLean JW, Thurston G, Roberge S, Jain RK and McDonald DM (2000) Openings between defective endothelial cells explain tumor vessel leakiness. *Am. J. Pathol.* **156**:1363-1380.
- Klein R, Klein BEK, Moss SE, Davis MD and DeMets DL (1984) The Wisconsin Epidemiologic Study of Diabetic Retinopathy. II. Prevalence and risk of diabetic retinopathy when age at diagnosis is less than 30 years. *Arch. Ophthalmol.* **102**:520-526.
- Kwak N, Okamoto N, Wood JM and Campochiaro PA (2000) VEGF is an important stimulator in a model of choroidal neovascularization. *Invest. Ophthalmol. Vis. Sci.* **41**:3158-3164.
- Liu C, Huang H, Donate F, Dickinson C, Santucci R, El-Sheikh A, Vessella R and Edgington TS (2002) Prostate-specific membrane antigen directed selective thrombotic infarction of tumors. *Canc. Res.* **62**:5470-5475.
- Liu H, Moy P, Kim S, Xia Y, Rajasekaran A, Navarro V, Knudsen B and Bander NH (1997) Monoclonal antibodies to the extracellular domain of prostate-specific membrane antigen also react with tumor vascular endothelium. *Canc. Res.* **57**:3629-3634.
- Liu Y, Cheung LH, Thorpe P and Rosenblum MG (2003) Mechanistic studies of a novel, human fusion toxin composed of vascular endothelial growth factor (VEGF)₁₂₁ and the serine protease granzyme B: Directed events in vascular endothelial cells. *Molec. Canc. Ther.* **2**:949-959.

Luna J, Tobe T, Mousa SA, Reilly TM and Campochiaro PA (1996) Antagonists of integrin alpha-v beta-3 inhibit retinal neovascularization in a murine model. *Lab. Invest.* **75**:563-573.

Nambu H, Nambu R, Melia M and Campochiaro PA (2003) Combretastatin A-4 Phosphate Suppresses Development and Induces Regression of Choroidal Neovascularization. *Invest. Ophthalmol. Vis. Sci.* **44**:3650-3655.

Nilsson F, Kosmehl H, Zardi L and Neri D (2001) Targeted delivery of tissue factor to the ED-B domain of fibronectin, a marker of angiogenesis, mediates the infarction of solid tumors in mice. *Canc. Res.* **61**:711-716.

Oh P, Li Y, Yu J, Durr E, Krasinska KM, Carver LA, Testa JE and Schnitzer JE (2004) Subtractive proteomic mapping of the endothelial surface in lung and solid tumours for tissue-specific therapy. *Nature* **429**:629-635.

Okamoto N, Tobe T, Hackett SF, Ozaki H, Viores MA, LaRochelle W, Zack DJ and Campochiaro PA (1997) Transgenic mice with increased expression of vascular endothelial growth factor in the retina: a new model of intraretinal and subretinal neovascularization. *Am. J. Pathol.* **151**:281-91.

Ozaki H, Seo M-S, Ozaki K, Yamada H, Yamada E, Hofmann F, Wood J and Campochiaro PA (2000) Blockade of vascular endothelial cell growth factor receptor signaling is sufficient to completely prevent retinal neovascularization. *Am. J. Pathol.* **156**:679-707.

- Pasqualini R, Koivunen E and Ruoslahti E (1997) Alpha v integrins as receptors for tumor targeting by circulating ligands. *Nat. Biotechnol.* **15**:542-546.
- Pasqualini R and Ruoslahti E (1996) Organ targeting in vivo using phage display peptide libraries. *Nature* **380**:364-366.
- Plate KH, Breier G, Millauer B, Ullrich A and Risau W (1993) Up-regulation of vascular endothelial growth factor and its cognate receptors in a rat glioma model of tumor angiogenesis. *Canc. Res.* **53**:5822-5827.
- Plate KH, Breier G, Welch HA and Risau W (1992) Vascular endothelial growth factor is a potential tumor angiogenesis factor in human gliomas *in vivo*. *Nature* **359**:845-848.
- Ramakrishnan S, Olson TA, Bautch VL and Mohanraj D (1996) Vascular endothelial growth factor-toxin conjugate specifically inhibits KDR/flk-1-positive endothelial cell proliferation *in vitro* and angiogenesis *in vivo*. *Canc. Res.* **56**:1324-1330.
- Ran S, Gao B, Duffy S, Watkins L, Rote N and Thorpe PE (1998) Infarction of solid Hodgkin's tumors in mice by antibody-directed targeting of tissue factor to tumor vasculature. *Canc. Res.* **58**:4646-4653.
- Saishin Y, Saishin Y, Takahashi K, Lima Silva R, Hylton D, Rudge J, J. WS and Campochiaro PA (2003) VEGF-TRAP_{R1R2} suppresses choroidal neovascularization and VEGF-induced breakdown of the blood-retinal barrier. *J. Cell. Physiol.* **195**:241-248.

Schnitzer JE (1998) Vascular targeting as a strategy for cancer therapy. *N. Eng. J. Med.* **339**:472-474.

Seo M-S, Kwak N, Ozaki H, Yamada H, Okamoto N, Fabbro D, Hofmann F, Wood JM and Campochiaro PA (1999) Dramatic inhibition of retinal and choroidal neovascularization by oral administration of a kinase inhibitor. *Am. J. Pathol.* **154**:1743-1753.

Shweiki D, Itin A, Soffer D and Keshet E (1992) Vascular endothelial growth factor induced by hypoxia may mediate hypoxia-initiated angiogenesis. *Nature* **359**:843-845.

Smith LEH, Wesolowski E, McLellan A, Kostyk SK, D'Amato R, Sullivan R and D'Amore PA (1994) Oxygen-induced retinopathy in the mouse. *Invest. Ophthalmol. Vis. Sci.* **35**:101-111.

Thorpe PE (2004) Vascular targeting agents as cancer therapeutics. *Clin. Canc. Res.* **10**:415-427.

Tobe T, Okamoto N, Viores MA, Derevjani NL, Viores SA, Zack DJ and Campochiaro PA (1998a) Evolution of neovascularization in mice with overexpression of vascular endothelial growth factor in photoreceptors. *Invest. Ophthalmol. Vis. Sci.* **39**:180-8.

Tobe T, Ortega S, Luna L, Ozaki H, Okamoto N, Derevjani NL, Viores SA, Basilico C and Campochiaro PA (1998b) Targeted disruption of the *FGF2*

gene does not prevent choroidal neovascularization in a murine model.

Am. J. Pathol. **153**:1641-1646.

Veenendaal LM, Jin H, Ran S, Cheung L, Navone N, Marks JW, Waltenberger J, Thorpe P and Rosenblum MG (2002) *In vitro* and *in vivo* studies of a VEGF₁₂₁/rGelolin chimeric fusion toxin targeting the neovasculature of solid tumors. *Proc. Natl. Acad. Sci. USA* **99**:7866-7871.

Verbeke G and Molenberghs G (2000) *Linear Mixed Models for Longitudinal Data*. Springer-Verlag, Inc., New York.

Zardi L, Carnemolla B, Siri A, Petersen TE, Paoletta G, Sebastio G and Baralle FE (1987) Transformed human cells produce a new fibronectin isoform by preferential alternative splicing of a previously unobserved exon. *EMBO J* **6**:2337-2342.

Figure Legends

Figure 1. VEGF receptor 2 is upregulated in choroidal and retinal neovascularization.

Adult C57BL/6 mice (n=6) had laser-induced rupture of Bruch's membrane in 10 locations in one eye and after 1 week, RNA was isolated from the eyecup of each eye. At postnatal day 16, rho/VEGF transgenic mice and littermate controls (n=6 for each) had RNA isolated from the retinas of one eye. Quantitative real time RT-PCR was done as described in Methods using primers specific for *VEGF receptor 2* (*VEGFR2*) mRNA and 28S rRNA. Bars represent the mean (\pm SEM) number of *VEGFR2* transcripts per 10^7 28S transcripts. There is a significant increase in *VEGFR2* mRNA in choroids containing choroidal neovascularization or in retinas containing retinal neovascularization.

Figure 2. Localization of VEGF/rGel in choroidal neovascularization after intravenous injection.

Adult C57BL/6 mice had laser-induced rupture of Bruch's membrane in each eye and after one week they were given a tail vein injection of PBS (A and B), 45 mg/kg of rGel (C and D), or 45 mg/kg of VEGF/rGel (E and F). One hour after the intravenous injections, mice were euthanized and eyes were removed and snap frozen. Ocular sections were histochemically stained with *Griffonia simplicifolia* lectin (GSA) visualized with diaminobenzidine (A, C, and E) or

immunohistochemically stained with anti-gelonin antibody using a fluorescein-labeled secondary antibody (B, D, and F).

(A) An ocular section of a mouse given an intravenous injection of PBS one week after rupture of Bruch's membrane shows GSA-stained choroidal neovascularization (arrows) at a rupture site.

(B) A section adjacent to the one shown in (A) immunofluorescently stained with anti-gelonin shows faint background staining throughout the retina with no increase in staining in the choroidal neovascularization (arrows).

(C) An ocular section of a mouse given an intravenous injection of rGel one week after rupture of Bruch's membrane shows GSA-stained choroidal neovascularization (arrows) at a rupture site.

(D) A section adjacent to the one shown in (C) immunofluorescently stained with anti-gelonin shows faint background staining throughout the retina with no increase in staining in the choroidal neovascularization (arrows).

(E) An ocular section of a mouse given an intravenous injection of VEGF/rGel one week after rupture of Bruch's membrane shows GSA-stained choroidal neovascularization (arrows) at a rupture site.

(F) A section adjacent to the one shown in (E) immunofluorescently stained with anti-gelonin shows faint background staining in the retina with staining above background throughout the choroidal neovascularization (arrows), indicating localization of the VEGF/rGel within the choroidal neovascularization.

Figure 3. Intravenous injection of VEGF/rGel causes regression of choroidal neovascularization.

Thirty adult C57BL/6 mice had laser-induced rupture of Bruch's membrane at three locations in each eye. After 1 week, 7 mice were perfused with fluorescein-labeled dextran and the baseline amount of choroidal neovascularization at rupture sites was measured by image analysis of choroidal flat mounts (A). The remaining mice were divided into three groups: 8 mice received a tail vein injection of 45 mg/kg of rGel every 2 days for a total of 4 injections (B), 7 mice received a tail vein injection of PBS every 2 days (C), and 8 mice received a tail vein injection of 45 mg/kg of VEGF/rGel every 2 days (D). After 1 week, the mice were perfused with fluorescein-labeled dextran and choroidal flat mounts were examined by fluorescence microscopy. The area of choroidal neovascularization at rupture sites appeared substantially smaller in mice that had been injected with VEGF/rGel (D, arrows) than those in mice that had been injected with rGel (B, arrows) or PBS (C, arrows). It was also smaller than the amount of choroidal neovascularization seen at baseline (A). Image analysis confirmed that the area of choroidal neovascularization was significantly smaller one week after injection of VEGF/rGel compared to baseline (E).

* $p = 0.0003$ for difference from baseline by linear mixed model

[†] $p < 0.0001$ for difference from gelonin by linear mixed model

Bar = 100 μ m

Figure 4. Intravitreal injection of VEGF/rGel causes regression of choroidal neovascularization.

Thirty-one C57BL/6 mice had laser-induced rupture of Bruch's membrane at three locations in each eye. After 1 week, 9 mice were perfused with fluorescein-labeled dextran and the baseline amount of choroidal neovascularization at rupture sites was measured by image analysis of choroidal flat mounts. The remaining mice were divided into 2 groups: 9 mice received an intravitreal injection of 5 ng of rGel in one eye and PBS in the fellow eye, and 13 mice received an intravitreal injection of 5 ng of VEGF/rGel in one eye and PBS in the fellow eye. After 1 week, the mice were perfused with fluorescein-labeled dextran and choroidal flat mounts were examined by fluorescence microscopy. There was a substantial amount of baseline choroidal neovascularization at 7 days after rupture of Bruch's membrane (A, arrows). At day 14, seven days after injection of rGel (B, arrows) or PBS (C, arrows), the area of choroidal neovascularization at rupture sites appeared similar to that seen at baseline (A). The amount of choroidal neovascularization seen 7 days after injection of VEGF/rGel (D, arrows) appeared less than that seen after injection of rGel or PBS, and less than that seen at baseline. Image analysis confirmed that the area of choroidal neovascularization was significantly smaller one week after injection of VEGF/rGel compared to injection of rGel or PBS, or the baseline amount (E).

* $p = 0.0009$ for difference from baseline by linear mixed model

[†] $p = 0.0002$ for difference from gelonin by linear mixed model

Bar = 100 μ m

Figure 5. Intravitreal injection of VEGF/rGel causes regression of subretinal neovascularization in rho/VEGF transgenic mice.

Several litters of hemizygous rho/VEGF transgenic mice were divided into 2 groups. The first group (n = 8) was perfused with fluorescein-labeled dextran at P21 and the baseline amount of neovascularization on the outer surface of the retina was measured by fluorescence microscopy and image analysis of retinal flat mounts. The second group (n = 9) received an intravitreal injection of 5 ng of rGel in one eye and 5 ng of VEGF/rGel in the fellow eye at P21. At P25, the mice were perfused with fluorescein labeled dextran and the area of neovascularization on the outer surface of the retina was measured.

(A) High magnification view of a retinal flat mount of a rho/VEGF mouse at P21 shows numerous tufts of neovascularization (arrows) partially surrounded by RPE cells. The retinal vessels are out-of-focus in the background.

(B) At P25, a retinal flat mount from an eye that received an intravitreal injection of rGel at P21 shows several tufts of neovascularization (arrows).

(C) At P25, a retinal flat mount from an eye that received an intravitreal injection of VEGF/rGel at P21 shows only one small remaining bud of neovascularization (arrow).

(D) Measurement of the area of subretinal neovascularization by image analysis showed that at P25, eyes injected with VEGF/rGel had less neovascularization

than eyes injected with rGel and less than the baseline amount of neovascularization at P21.

* $p < 0.0001$ for difference from baseline by linear mixed model

[†] $p < 0.0001$ for difference from gelonin by linear mixed model

Bar = 100 μ m

Figure 6. Intravitreal injection of VEGF/rGel causes regression of ischemia-induced retinal neovascularization.

Mice were placed in 75% oxygen at P7 and at P12 they were removed to room air. At P17, the baseline amount of neovascularization was measured (n=6) and the remaining mice (n=7) were given an intravitreal injection of 5 ng of VEGF/rGel in one eye and 5 ng of rGel in the fellow eye. At P21, ocular sections stained with *Griffonia simplicifolia* lectin showed prominent baseline neovascularization on the surface of the retina in P17 mice (A and B, arrows). Substantial neovascularization was also seen at P21 in eyes that had been injected with rGel (C and D, arrows), but almost no neovascularization was detectable in eyes that had been injected with VEGF/rGel (E and F, arrow). Measurement of the area of retinal neovascularization by image analysis showed that at P21 eyes injected with VEGF/rGel had less neovascularization than that seen in eyes injected with rGel and less than the baseline neovascularization at P17 (G).

* $p < 0.0001$ for difference from baseline by linear mixed model

[†] $p < 0.0001$ for difference from gelonin by linear mixed model

Bar = 100 μ m

Fig.1

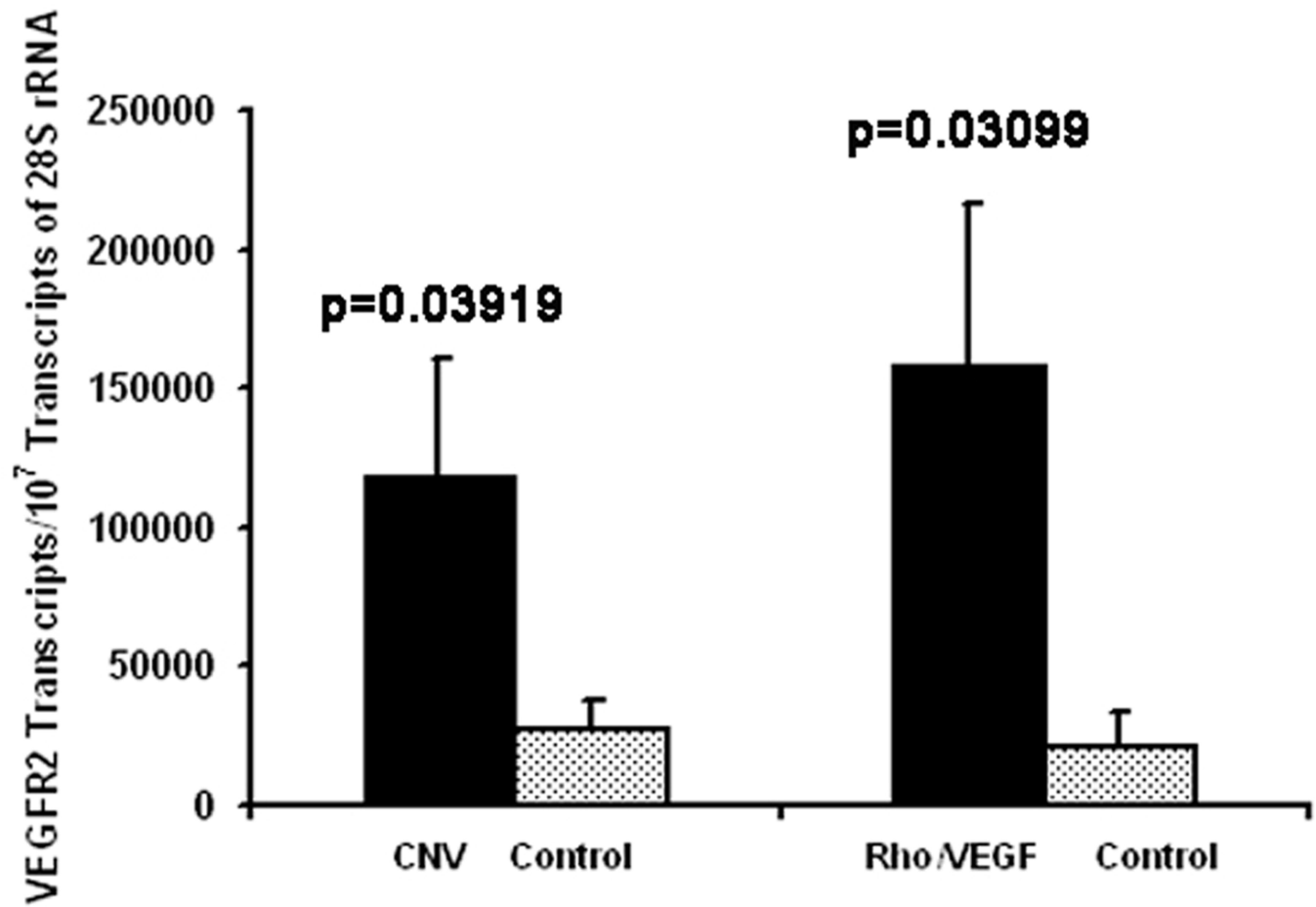


Fig.2

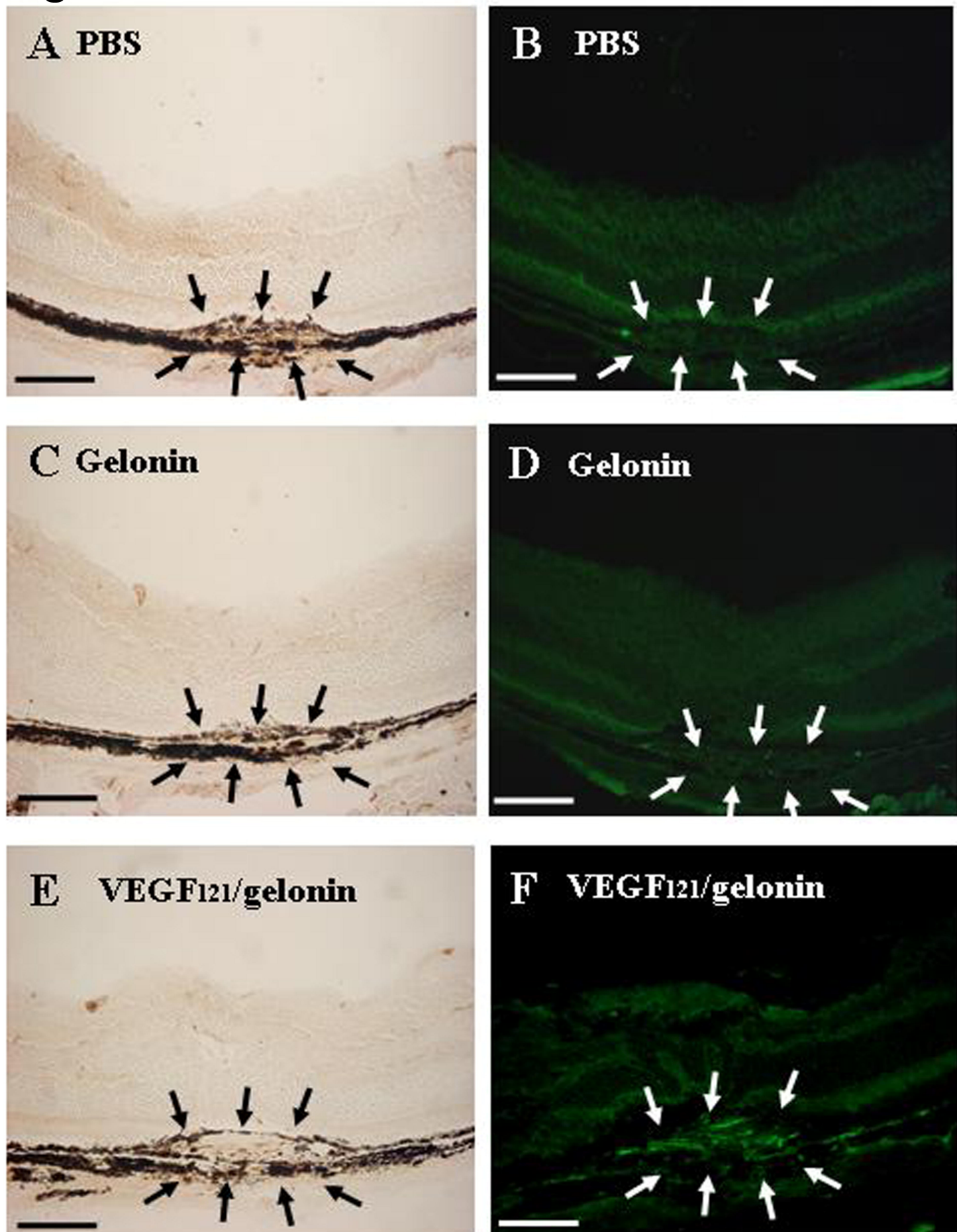
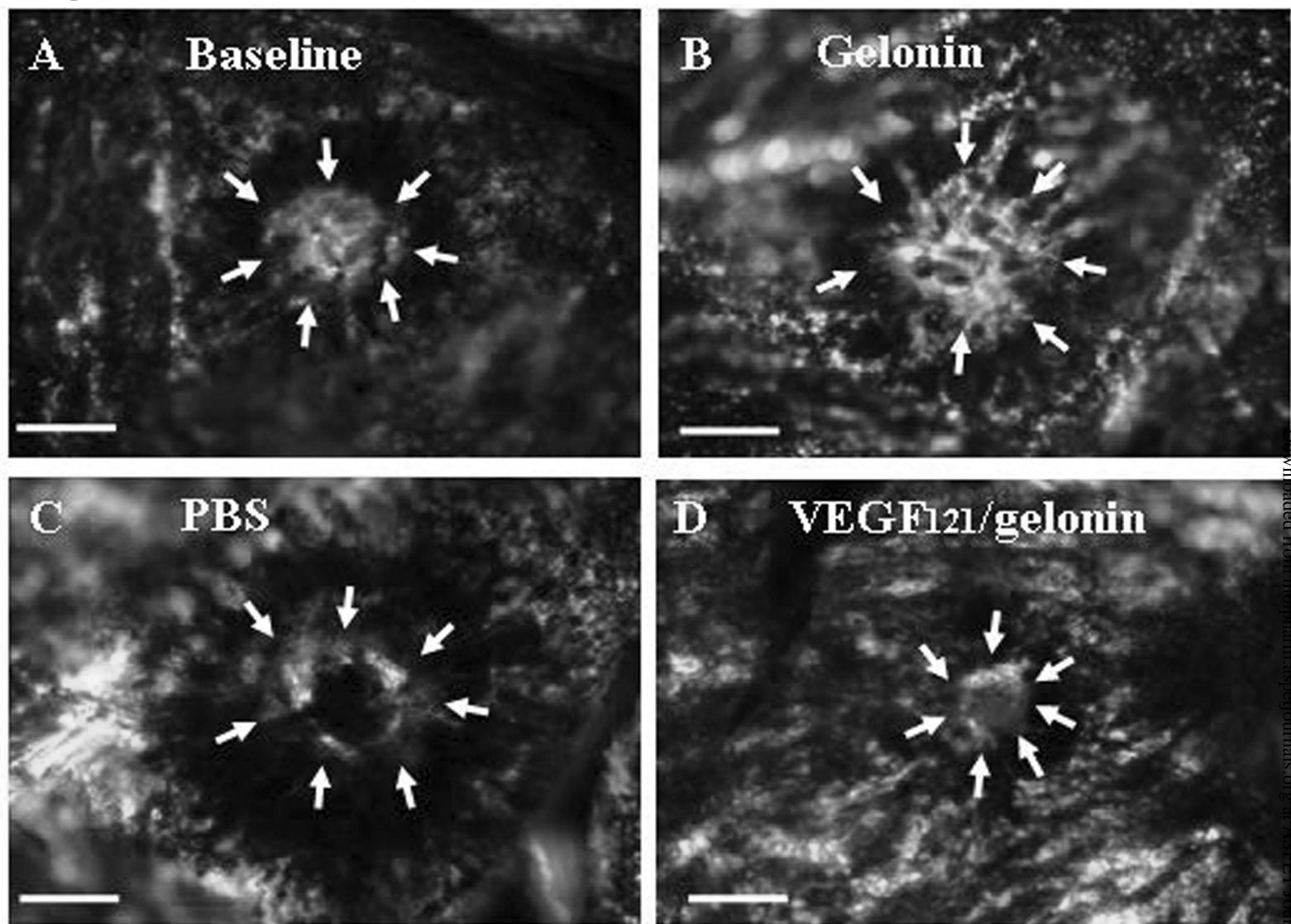


Fig.3



E

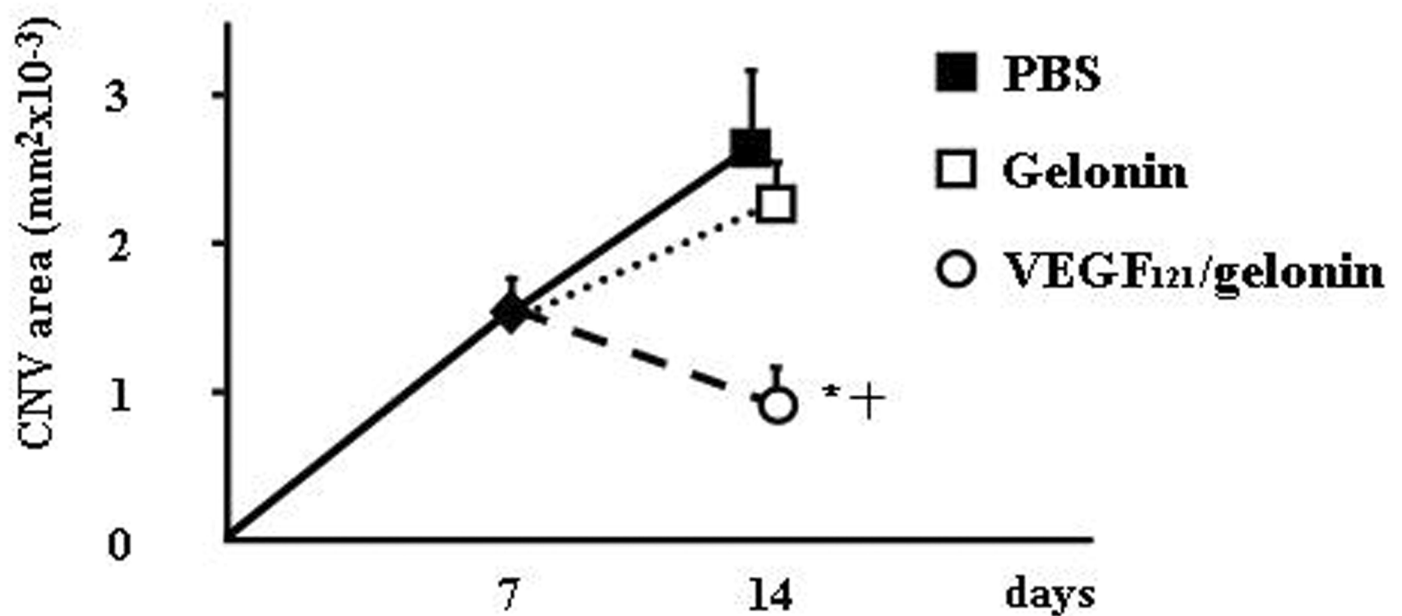
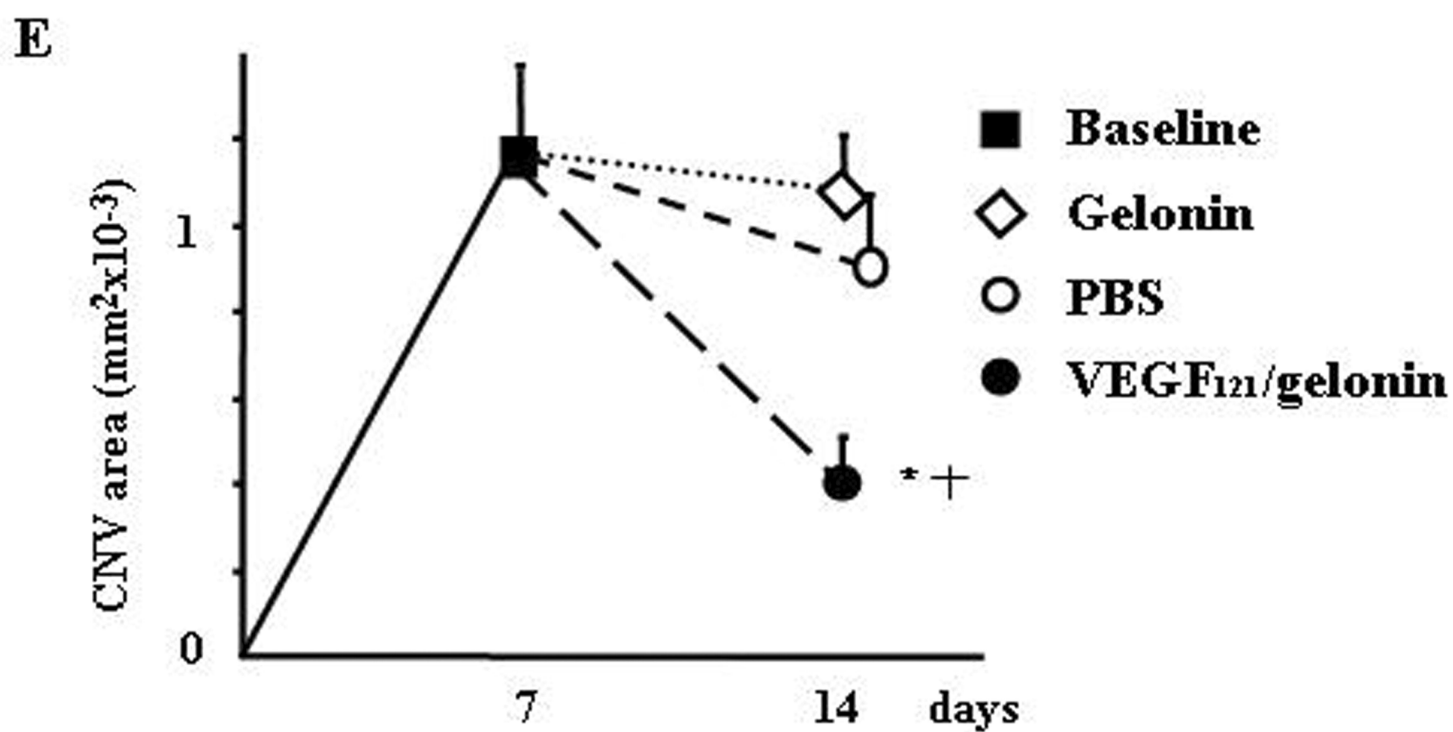
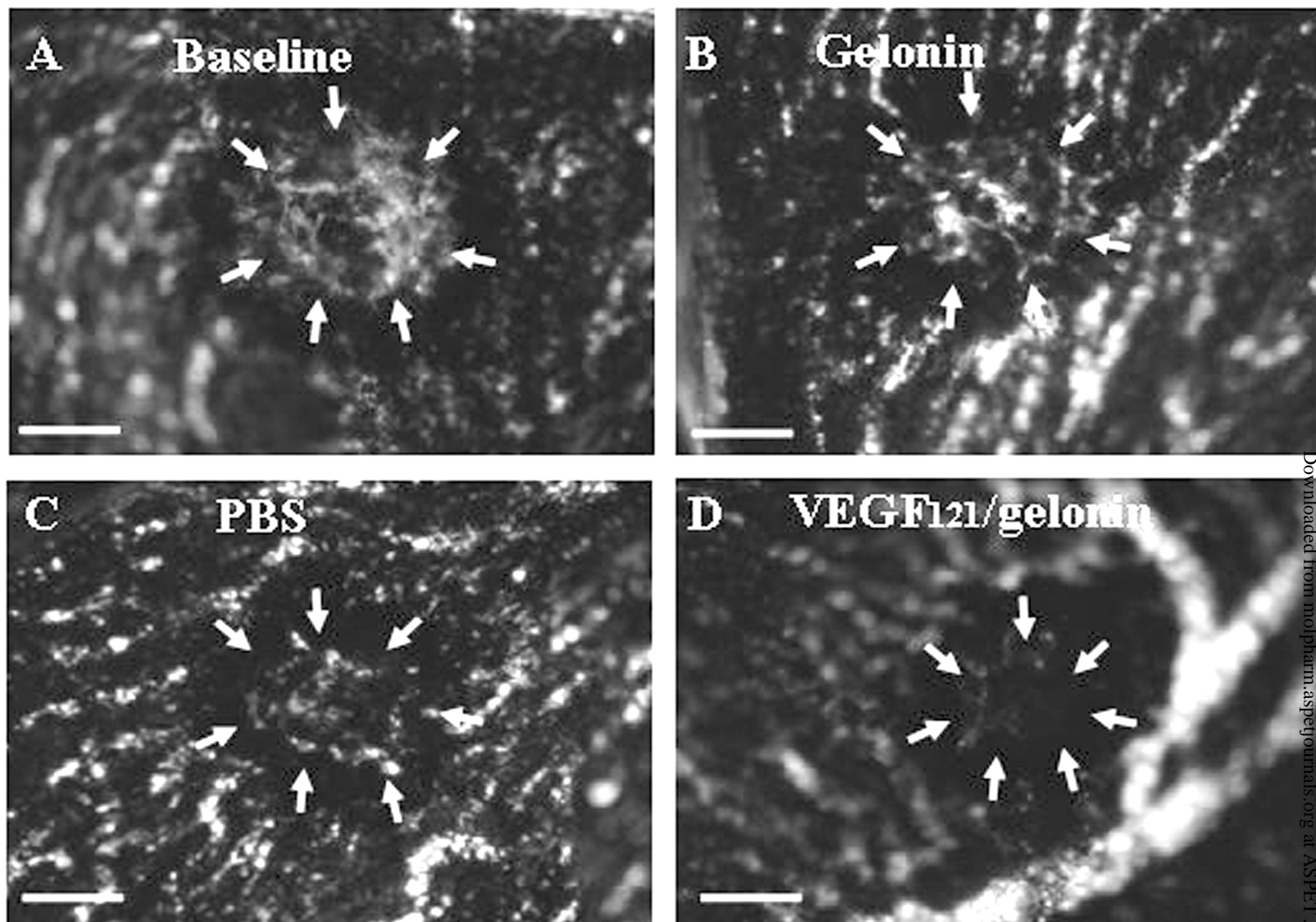


Fig.4



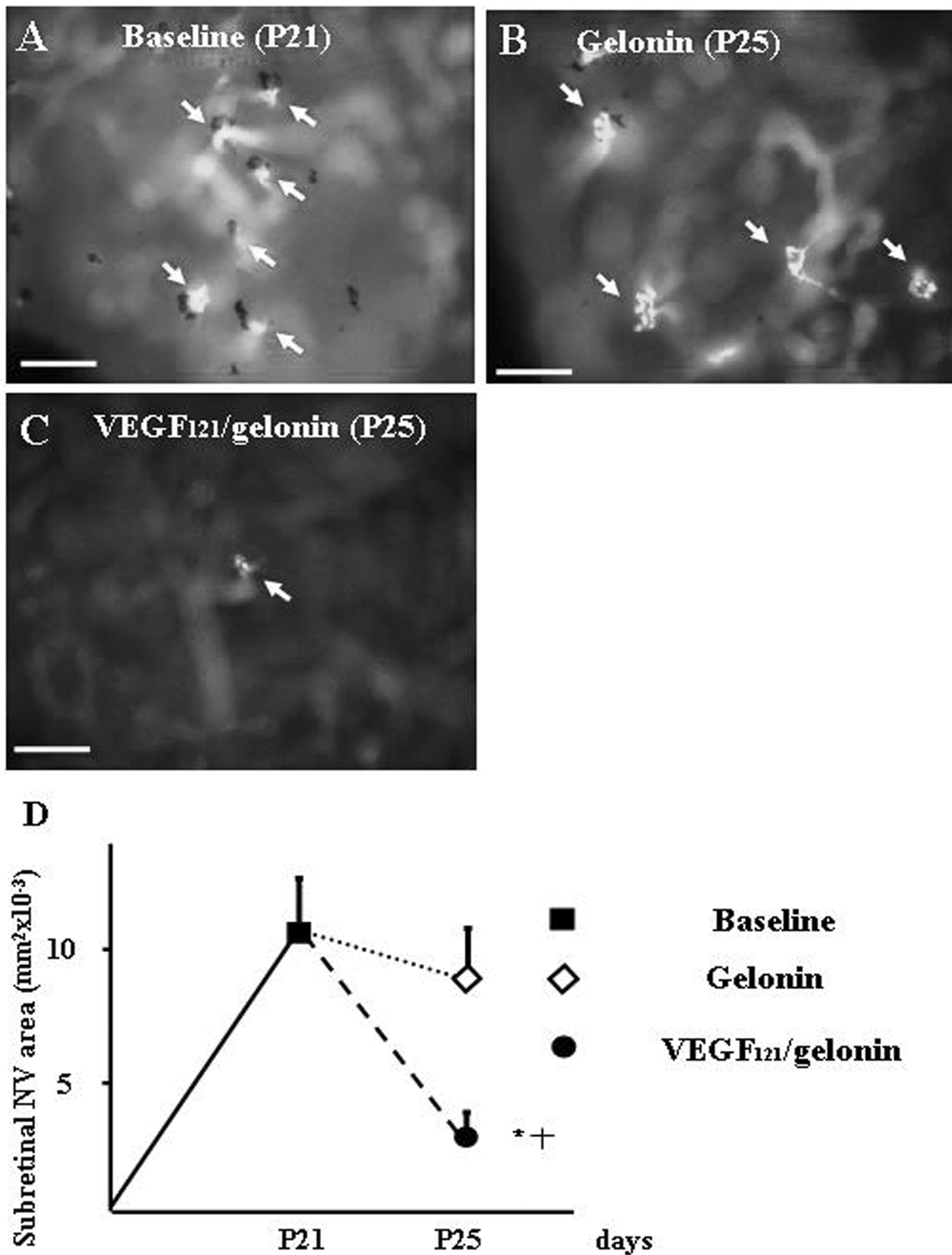


Fig.6

